(Appeared in *Exploration Geophysics*, **45**, 24-36, 2014)
DOI: http://dx.doi.org/10.1071/EG13041

Aeromagnetic constraints on the subsurface structure of Usu Volcano, Hokkaido, Japan

Shigeo Okuma[1] Tadashi Nakatsuka Yoshihiro Ishizuka

Geological Survey of Japan, AIST, AIST Tsukuba Centerl 7, Higashi 1-1-1, Tsukuba 305-8567, Japan

[1] E-mail: s.okuma@aist.go.jp

Key Words: aeromagnetic survey, lava, magnetic anomaly, Usu Volcano, volcanic rocks.

Abstract

Usu Volcano, Hokkaido, Japan consists mainly of dacitic volcanic rocks underlain by basaltic somma lava and Pliocene–Pleistocene andesitic volcanic rocks, and erupts every 20–30 years. The most recent eruption, in 2000, was the first since 1978. We conducted a helicopter-borne high-resolution aeromagnetic survey almost three months after the start of this eruption. We calculated magnetic anomalies on a smoothed observation surface using a reduction method, assuming equivalent anomalies below the actual observation surface. We conducted three-dimensional (3D) imaging of magnetic anomalies to constrain the subsurface structure. Our model indicates that there are magnetisation highs in the main edifice of Usu Volcano, which may reflect the subsurface distribution of the Usu somma lava. Meanwhile, magnetisation lows lie northwest of the Nishi-Yama Craters Area and on Higashi-Maruyama Cryptodome, where nearby Pliocene and Pleistocene volcanic rocks, respectively, are found. The reverse magnetisation observed at outcrops close to these sites could explain the magnetisation lows.

Although the survey improved our understanding of the surface and subsurface distribution of volcanic rocks in the edifice and basement of Usu Volcano, some limitations remain. No information about the magmas intruded during the recent eruptions in 1977–1978 and 2000 was obtained by the survey, though some of these intrusions were revealed by other geophysical data. The small magnetic contrast between the intruded magmas and their host rocks is the most probable reason. Perhaps the intruded magmas (in particular, those of the most recent eruption) had not cooled enough to become strongly magnetised by the time the survey was conducted.

Introduction

On 31 March 2000, Usu Volcano, Hokkaido, Japan erupted for the first time since an eruption in 1977–1978. A few months after this eruption began, in June 2000, we carried out a helicopterborne aeromagnetic survey to monitor the eruptive activity, because the eruption was very intense at the beginning (Okuma et al., 2001, 2002, 2010; Figure 1). Successive repeat aeromagnetic surveys separated by several months were also planned at first but were not conducted because the major activity of the eruption paused from June until September 2000. The observed survey data were processed and magnetic anomalies were reduced onto a smoothed observed surface, which was used to compile an aeromagnetic anomaly map, published on a scale of 1:25 000 (Okuma et al., 2003).

In this area, no detailed aeromagnetic surveys had been conducted before the 2000 eruption. Instead, intensive ground magnetic surveys had been conducted by Nishida and Miyajima (1984). They analysed observed magnetic anomalies, using the assumption that the volcanic structure is an ensemble of simple circular cones. Their analysis indicated that the main body of the Usu Volcano comprises strongly magnetised basaltic soma lavas (10 A/m) and weakly magnetised crater fill (3 A/m). They proposed a general concept of the subsurface structure of the volcano. However, the limited number of magnetic stations in place did not allow for detailed analyses except for the Showa-Shinzan Lava Dome, where the temperature of some parts of the lava dome was inferred to be above the Curie temperature through magnetic modelling (Nishida and Miyajima, 1984).

To further the existing studies in this area, we conducted three-dimensional (3D) imaging of aeromagnetic anomalies of the area to better understand the shallow subsurface structure of the volcano. In this paper, we explain detailed characteristics of magnetic anomalies found in the area and discuss the subsurface structure deduced from this 3D magnetic imaging.

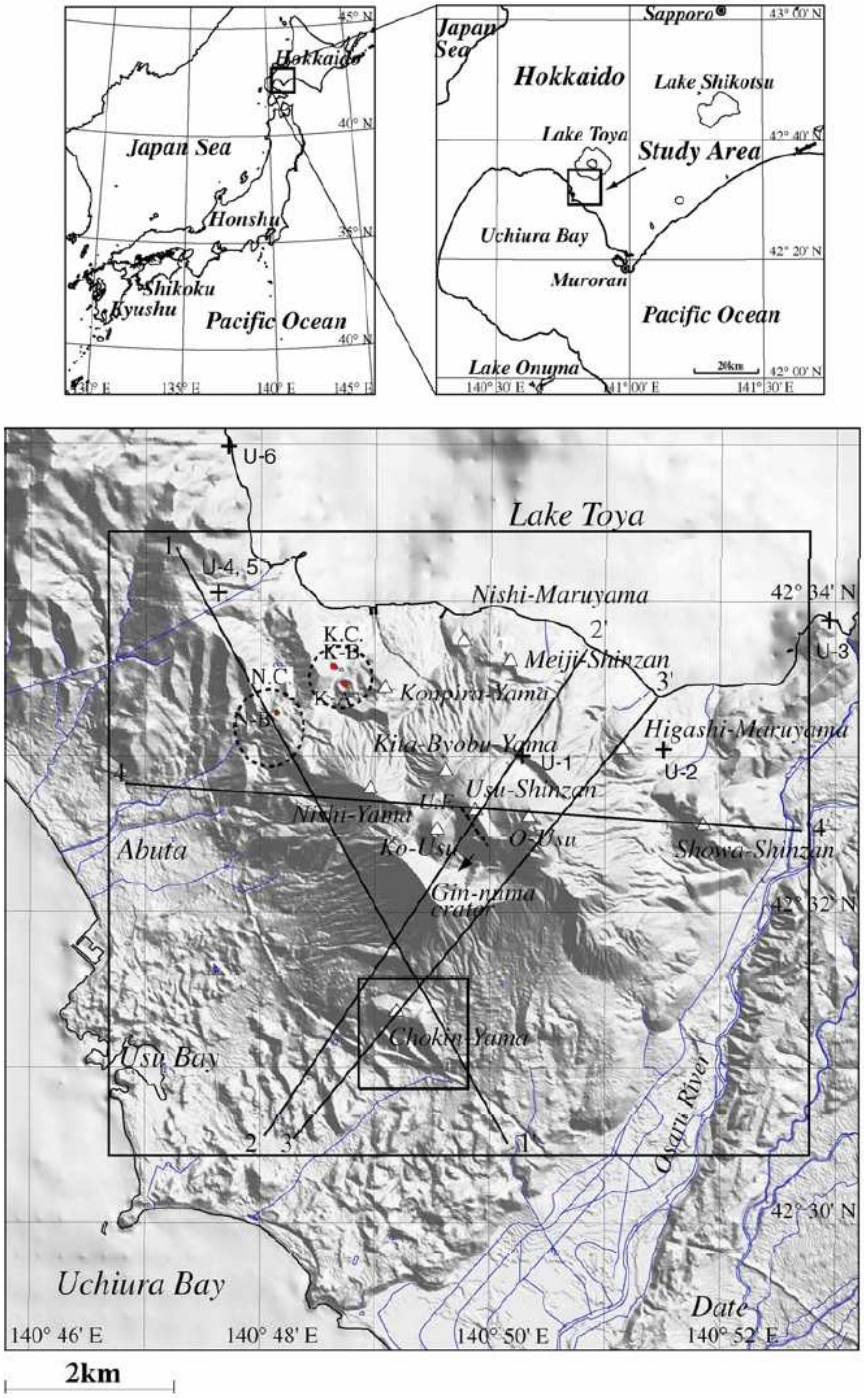

Fig. 1. Location map of the study area. Topographic shading has been superimposed. DEMdata with 10m and 50m mesh (Geospatial Information Authority of Japan, 1999, 2007) were employed to produce this map. K.C. and the corresponding circle with a dashed-and-dotted outline indicate the location of the Kompira-Yama craters. N.C. and the corresponding circle with a dashed-and-dotted outline indicate the location of the Nishi-Yama craters. K-A and K-B in the Kompira-Yama craters (K.C.) and N-B in the Nishi-Yama craters (N.C.) were active craters during the survey. U.F. and the corresponding dashed line show the location of the Usu-Shinzan fault (Katsui et al., 1985). An arrow shows the location of Gin-numa crater. White triangles indicate summits of mountains. U-1–U-6 indicate locations of rock sampling sites. The entire area corresponds to that of the high resolution aeromagnetic survey. The inner rectangle shows the airborne EM survey area. Thick solid lines represent the locations where cross-sections of magnetic structure were generated. The small rectangle denotes the detailed study area of Chokin-Yama and its surroundings (Figure 8*a*).

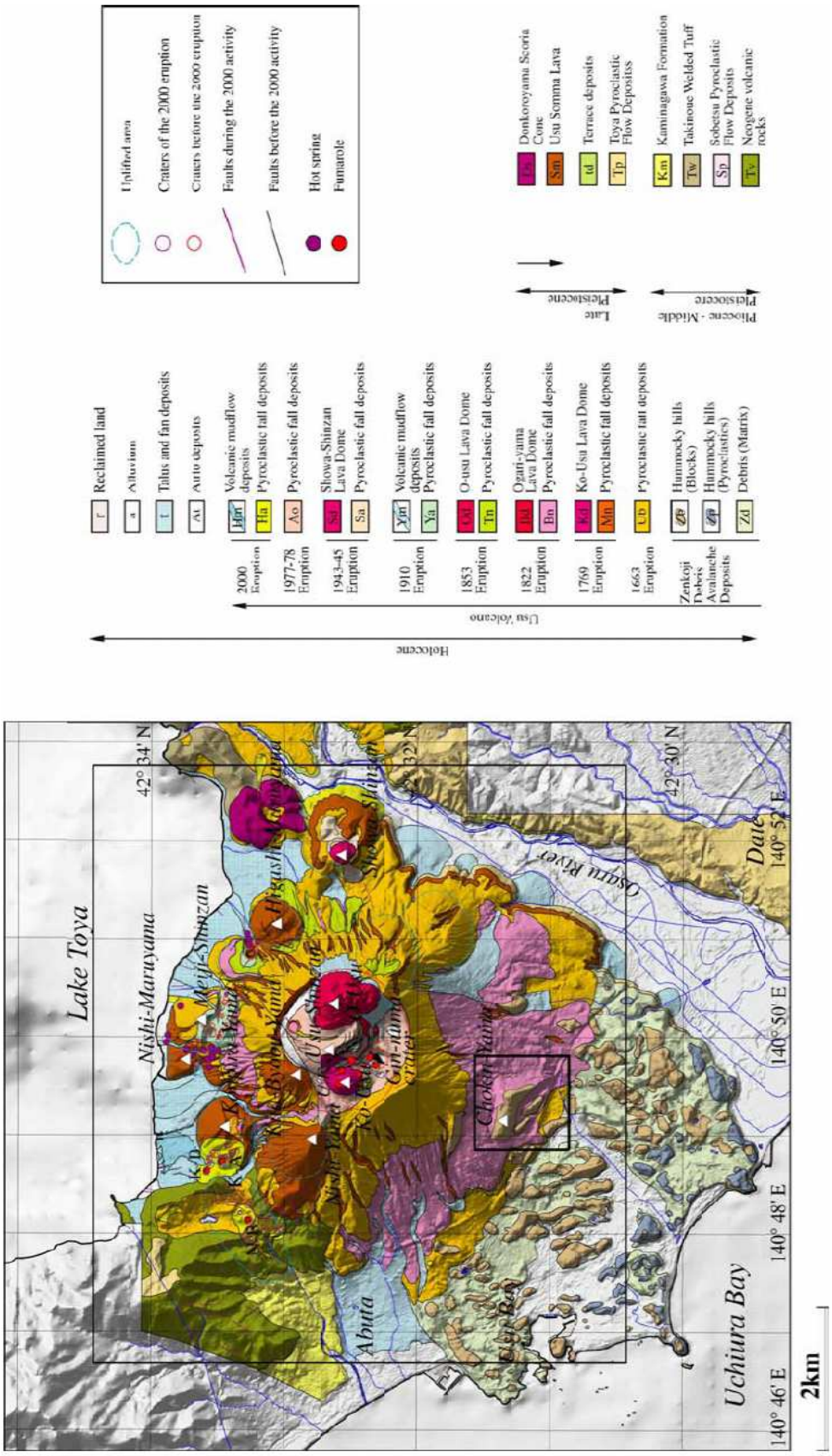

Fig. 2. A simplified geologic map of Usu Volcano, Hokkaido, Japan, modified from Soya et al. (2007). The small rectangle denotes the detailed study area of Chokin-Yama and its surroundings (Figure 8*a*).

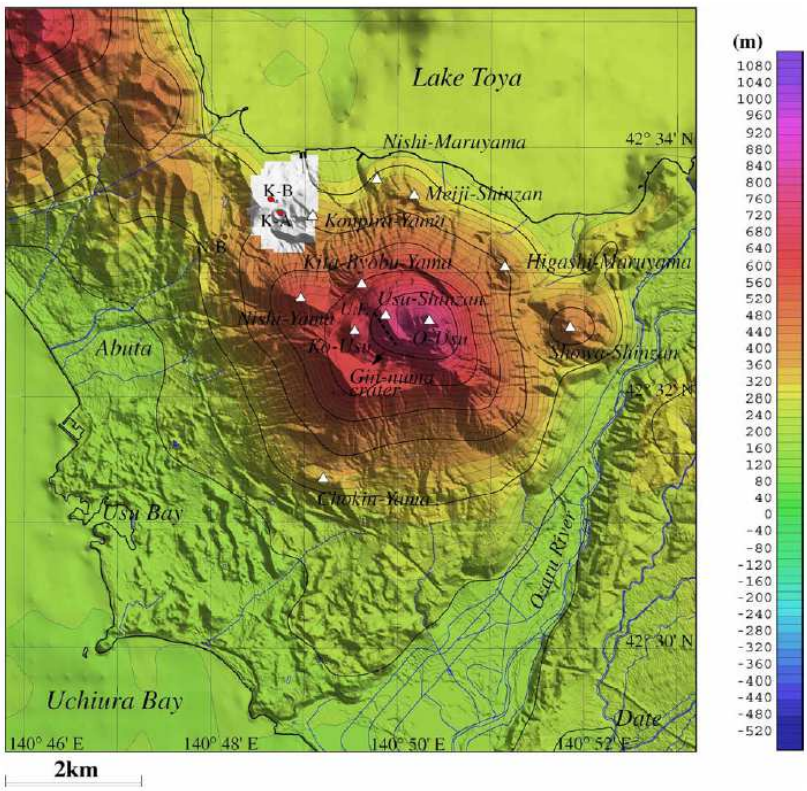

Fig. 3. The smoothed observed surface calculated from flight lines of the survey. The contour interval is 20 m. Flight line paths of the high-resolution aeromagnetic survey over Usu Volcano are superimposed.

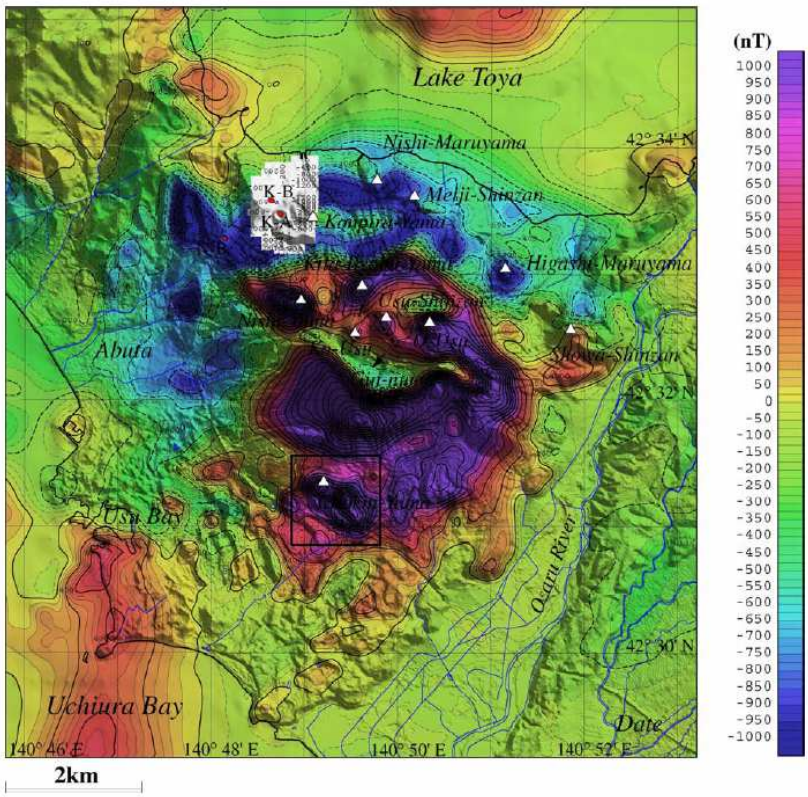

Fig. 4. Total magnetic intensity anomaly map of Usu Volcano. Contour interval is 50 nT. Dashed contours indicate negative values. The small rectangle denotes the detailed study area of Chokin-Yama and its surroundings (Figure 8*a*).

Geology

Usu Volcano is a Quaternary volcano, located at the southern edge of the Toya Lake in southern Hokkaido, facing the Pacific Ocean to the south (Figure 2). The volcano consists mainly of basalt and basalt-andesite somma lava, with some dacite lava domes and cryptodomes, and erupts every 20–30 years (Soya et al., 2007). The initiation of the volcano has not yet been dated, but is believed to be around 10 000 years ago. About 7000 or 8000 years ago, the summit of the main edifice collapsed and rushed down to the Pacific Ocean on the southern slope, forming the Zenkoji Debris Avalanche Deposits on the way. This volcano is very active: since an eruption in 1663, at least eight eruptions, including the 2000 eruption, have been observed. Most eruptions began with pyroclastic flows and terminated with lava-dome and/or cryptodome formation such as Ko-Usu and O-Usu inside the summit crater and Showa-Shinzan on the eastern foot during the 1943–1945 eruption. Since the start of the 20th century, four eruptions are known to have occurred, including the 2000 one. In 1910, phreatic eruptions occurred, creating many small craters at the northern foot of the main edifice of Usu Volcano and forming cryptodomes including Meiji-Shinzan. The 1943–1945 eruptive activity began with volcanic tremors at the eastern foot of the volcano in 1943. This was followed by phreatic eruptions in 1944, and the eruption terminated with the formation of Showa-Shinzan Lava Dome. The 1977–1978 eruption began with a pumice eruption in the summit crater area, which produced significant ash deposits that, in turn, caused volcanic mudflows. This pumice eruption was followed by crustal movements punctuated by an earthquake swarm, and also by formation of lava and cryptodomes including Usu-Shinzan Cryptodome. In 2000, phreatomagmatic and phreatic eruptions occurred, forming more than sixty minor craters at the north-western foot of the volcano. These were followed by the formation of Heisei-Shinzan Cryptodome and the initiation of new geothermal activity in the Nishi-Yama Craters Area.

Usu Volcano is underlain by Pliocene–Pleistocene volcanic rocks, which crop out in the north-west (Nottoko Lava, Tsukiura Lava (Ohta, 1956)) and north-east (Takinoue Pyroclastic Flow Deposits) of the volcano (Soya et al., 2007). These volcanic rocks are underlain by altered Neogene volcaniclastic rocks, which have been confirmed at depths ranging from a few hundred metres to a kilometre in drill holes around the volcano (Yahata, 2002).

Aeromagnetic survey and magnetic anomalies

A helicopter-borne high-resolution aeromagnetic survey was conducted in late June 2000, almost 3 months after the eruption began (Okuma et al., 2001). The survey was flown at an altitude of 150m above the terrain along north–south survey lines and east–west tie lines, spaced 200m and 1000m apart, respectively. A differential global positioning system (DGPS) with an accuracy of 50 cm was employed for flightpath recovery. Total magnetic intensity was observed every 0.1s and anomalies were calculated by subtracting the International Geomagnetic Reference Field (IGRF-10 (Maus et al., 2005)) from the observed values (Okuma et al., 2010). We reduced these aeromagnetic anomalies onto a smoothed observed surface (Figure 3), using the method of Nakatsuka and Okuma (2006*a*) in the space domain to compile a total magnetic intensity anomaly map (Figure 4). We also created some filtered maps, such as reduction to the pole (Figure 5).

The characteristics of the distribution of reduction to the pole anomalies can be summarised as follows:

1) Regional magnetic lows lie to the northwest of the 2000 eruption areas. Neogene volcanic rocks that are distributed in the area, and their known reversed magnetisation, may be responsible for these magnetic lows.
2) No apparent magnetic features can be seen in the Nishi-Yama Craters Area, one of the two active crater areas when the survey was conducted, though the area was uplifted by ~70 m after the eruption. This implies that the shallow intruded magma was not cool enough (i.e. probably above the Curie temperature) to cause magnetic anomalies.
3) Magnetic highs are distributed over lava domes such as O-Usu, Ko-Usu, and Showa-Shinzan, and over cryptodomes such as Nishi-Yama and Usu-Shinzan, showing that the volcanic rocks comprising those domes contain magnetic minerals and are cool enough to acquire magnetism.
4) Magnetic highs occupy the main edifice of Usu Volcano, suggesting that there is a subsurface distribution of the Usu somma lava, which is overlain by pyroclastic rocks.
5) Chains of magnetic highs are distributed over the south and south-western flanks of the main edifice of the volcano. Their positions correspond well to the distribution of the Zenkoji Debris Avalanche Deposits, which were formed by a summit collapse about 7000–8000 years ago. This does not necessarily imply that the debris avalanche deposits

were emplaced above the Curie temperature and magnetized thereafter. Their contribution to magnetic anomalies may originate only from their magnetic susceptibilities, even though their directions of magnetisation would be randomly oriented in this case, as a result of free rotation of the deposits while spreading on the flank. The extension of magnetic highs near Usu Bay indicates that the debris avalanche deposits reached the sea here. This is the second case where the distribution of debris avalanche deposits has been recognised as magnetic highs on aeromagnetic maps, following the case at the northern foot of Chokai Volcano, north-east Japan (Okuma et al., 1995).

Three-dimensional (3D) magnetic imaging

To identify the depth of the magnetic structure, we conducted 3D magnetic imaging (Nakatsuka and Okuma, 2009) as a 3D extension of the 2D magnetisation intensity mapping method (Nakatsuka, 1995).

Using vector/matrix notation, the magnetic anomaly $\boldsymbol{f}$ at an observation point is expressed as follows:

$$\boldsymbol{f} = \boldsymbol{A}\boldsymbol{s} \quad (1)$$

where $\boldsymbol{f}$ is the magnetic anomaly, $\boldsymbol{A}$ is a geometric factor, and $\boldsymbol{s}$ is magnetisation of the source.

Nakatsuka and Okuma (2006*b*) solved the equation using the conjugate gradient (CG) method. The simple CG method searches for the condition:

$$(\boldsymbol{f} - \mathbf{A}\boldsymbol{s})^{\mathrm{T}}(\boldsymbol{f} - \mathbf{A}\boldsymbol{s}) \rightarrow \mathrm{Min} \quad (2)$$

In order to regularise the method, another term is added in the minimising function as:

$$(\boldsymbol{f} - \mathbf{A}\boldsymbol{s})^{\mathrm{T}}(\boldsymbol{f} - \mathbf{A}\boldsymbol{s}) + e(\mathbf{B}\boldsymbol{s})^{\mathrm{T}}(\mathbf{B}\boldsymbol{s}) \rightarrow \mathrm{Min} \quad (3)$$

where $\boldsymbol{B}$ is the penalising operator matrix, and e is a tradeoff parameter (so-called hyper-parameter) to adjust the penalising weight ratio between the former misfit term $(\boldsymbol{f}-\boldsymbol{A}\boldsymbol{s})^{\mathrm{T}}(\boldsymbol{f}-\boldsymbol{A}\boldsymbol{s})$ and the latter regularisation term $R=(\boldsymbol{B}\boldsymbol{s})^{\mathrm{T}}(\boldsymbol{B}\boldsymbol{s})$ in equation 3.

In the case of a model composed of variable volume bodies (Nakatsuka and Okuma, 2009), the penalising operator and the regularising factor should be

$$\mathbf{B} = \mathrm{diag}\left\{\sqrt{\frac{v_i}{s_i^{\,2} + \delta^2}}\right\} \quad (4)$$

$$R = (\mathbf{B}\boldsymbol{s})^{\mathrm{T}}(\mathbf{B}\boldsymbol{s}) = \sum_i \frac{v_i\, s_i^{\,2}}{s_i^{\,2} + \delta^2} \quad (5)$$

where *vi* is volume of the *i*th body, and d is the critical value of magnetisation. As mentioned in the previous section, the detailed characteristics of the magnetic anomalies in the study area were revealed by a high-resolution aeromagnetic survey. They revealed the heterogeneity of the subsurface structure of the volcano arising from phenomena such as lava domes and cryptodomes surrounding the main edifice of the Usu Volcano. These geologic features cannot be sufficiently modelled by estimations using simple structural models such as a concentric cone (Nishida and Miyajima, 1984). To better estimate the detailed structure of the volcano, we applied 3D magnetic imaging to the observed total magnetic intensity anomalies (Figure 4), allowing 3D variations of the magnetisation intensity. The magnetic model with a flat bottom is composed of magnetic layers with constant thicknesses varying from 100 m to 250 m, except the uppermost one, and each layer consists of an ensemble of prism models with a horizontal dimension of 100 m by 100 m. The bottom depth of the magnetic structure was assumed to be 1 km below sea level, on the basis of a geologic interpretation that shows that fresh Quaternary and Neogene volcanic rocks are underlain by altered Neogene volcaniclastic rocks that have been confirmed at depths ranging from a few hundred metres to a kilometre in drill holes around the volcano (Yahata, 2002).

The iterative procedure of the imaging method was initiated using a uniform magnetisation of 4.4 A/m as the starting value, which was derived from the average terrain magnetisation. It was terminated when the root mean square of residuals of the observed and calculated field was 3.2 nT. Figures 6 and 7 show depth slices and cross-sections, respectively, from the imaging. Additional information such as reduction to the pole anomalies, apparent resistivities, gravity basement depths, and precursory seismic activity of the Usu 2000 eruption were superimposed on Figure 7 (Okuma et al., 2010).

Figure 7*a* shows the cross-section that traverses the Nishi-Yama Craters Area, one of the eruption areas in 2000. A local apparent resistivity low lies there, corresponding to fumarole activity that started soon after the 2000 eruption, probably arising from magma intrusions at shallow depth, and lasted more than 10 years. No apparent magnetic characteristics can be seen there, except for the existence of a boundary between normal (1–2 A/m) and reversed (~–10 A/m) magnetisation parts. Magnetisation highs (~8 A/m) were imaged below the southwestern and southern flank of Usu Volcano and correspond to the distribution of the Usu somma lava (Soya et al., 2007). Apparent resistivity highs also occupy the area.

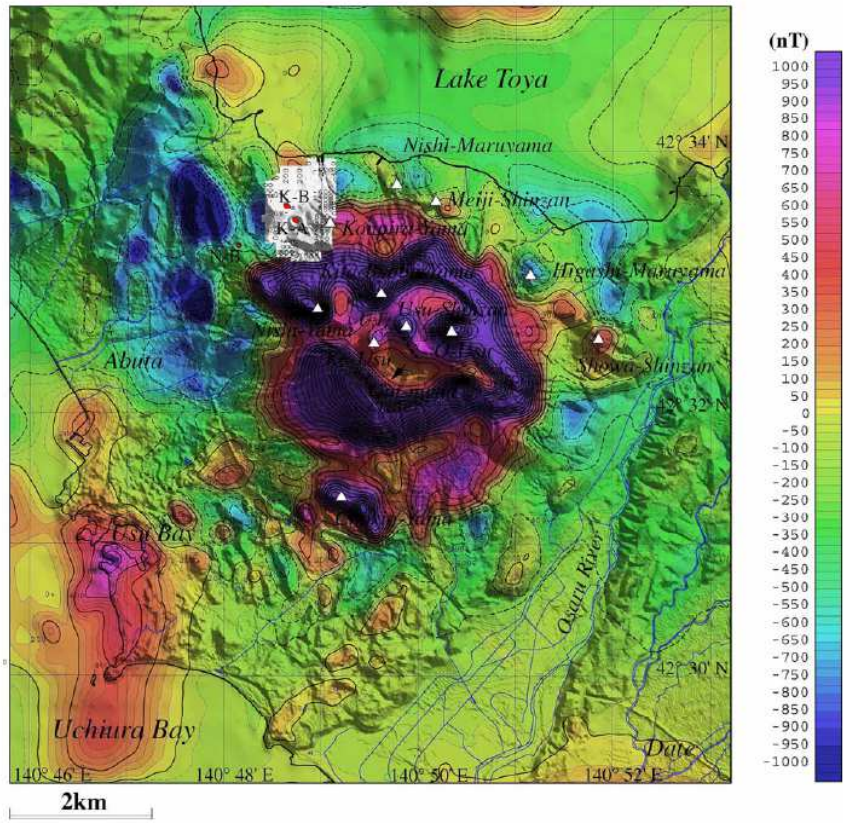

Fig. 5.
Reduction to the pole magnetic anomaly map of Usu Volcano. Contour interval is 50 nT. Dotted contours indicate negative values.

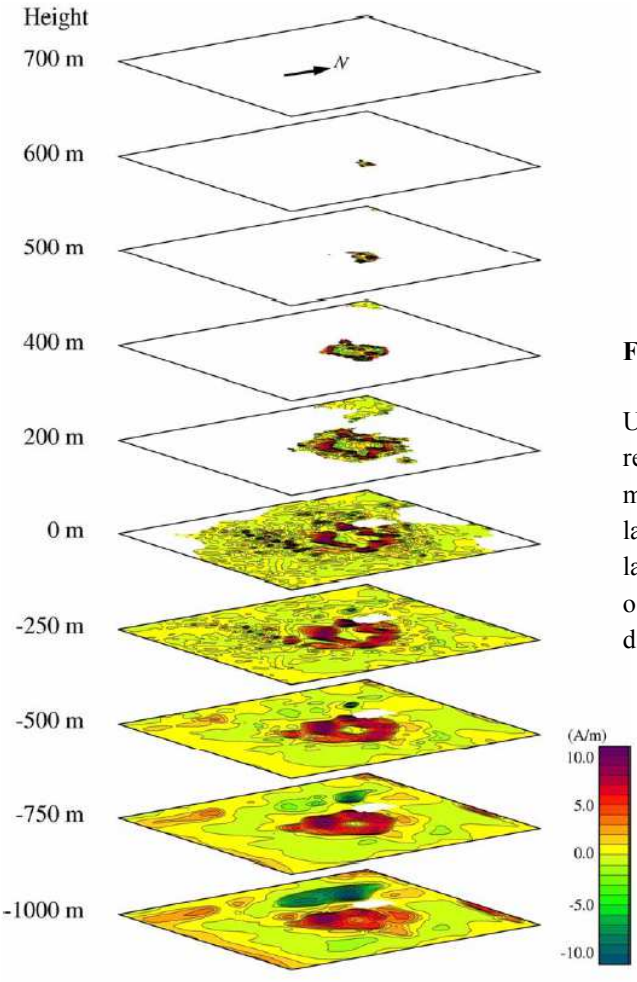

Fig. 6.
Depth slices of the result of 3D magnetic imaging of Usu Volcano and its vicinity. The depths in the map represent the bottom depths of each layer. The magnetic model with a flat bottom is composed of 10 magnetic layers with a constant thickness of 100m to 250m for all layers except the uppermost one, and each layer consists of an ensemble of prism models with horizontal dimensions of 100 m by 100 m.

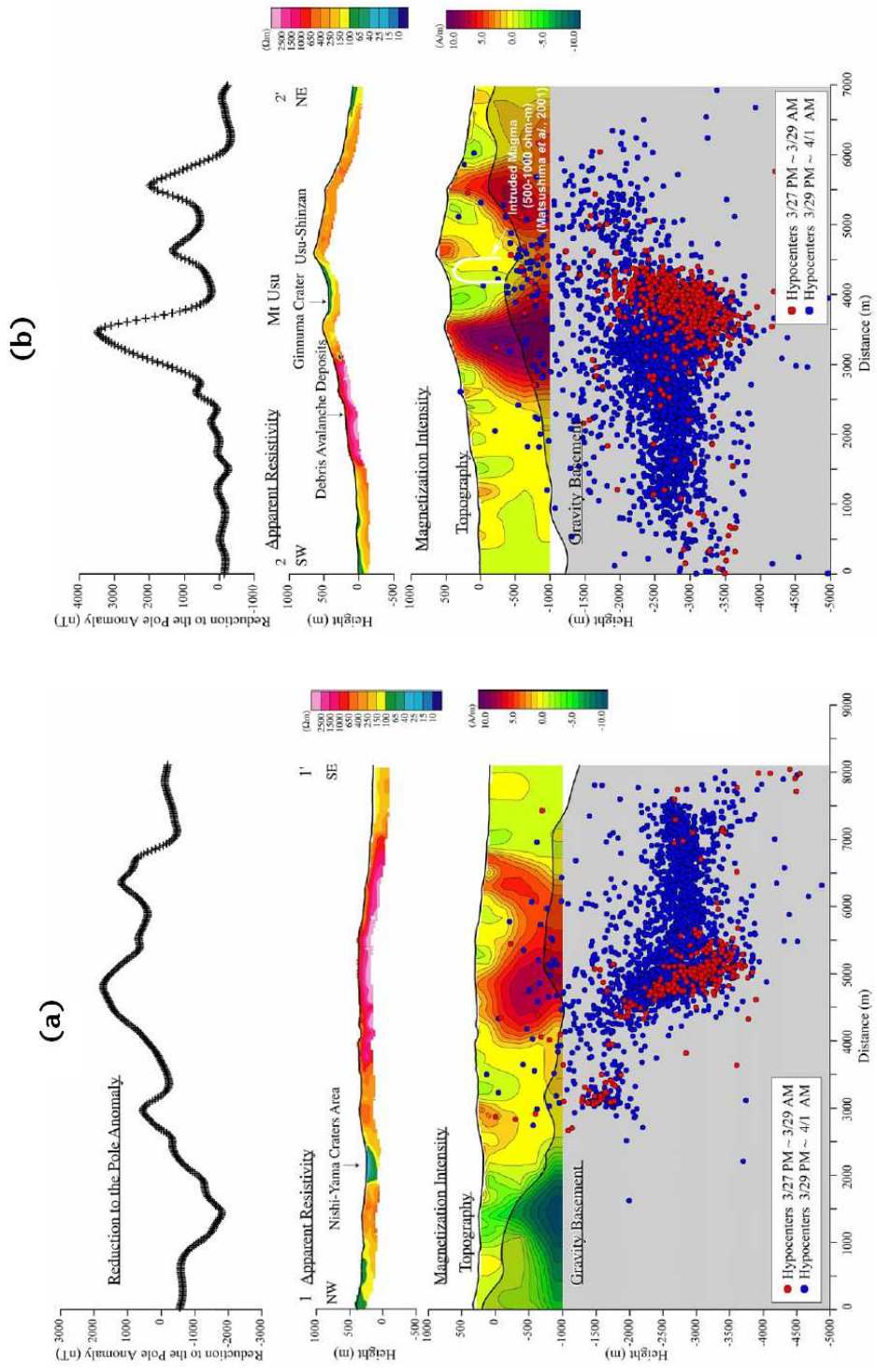

Fig. 7. (*a*) Cross-sections of the magnetic structure along the profile of 1–1'. The contour interval of magnetisation intensity is 1.0 A/m. Reduction to the pole anomalies, apparent resistivities, and gravity basement depths are superimposed from the top to the bottom (Okuma et al., 2010). Red and blue circles denote the hypocentres (Onizawa, 2010) from the afternoon of 27 March 2000 to the morning of 29 March 2000, and from the afternoon of 29 March 2000 to the morning of 1 April 2000, respectively. See the location of the profile on Figure 1. (*b*) Cross-sections of the magnetic structure along the profile of 2–2'. A resistivity cross-section from the MT survey (Matsushima, 2010) is superimposed on this section. (*c*) Cross-sections of the magnetic structure along the profile of 3–30. (*d*) Cross-sections of the magnetic structure along the profile of 4–4'.

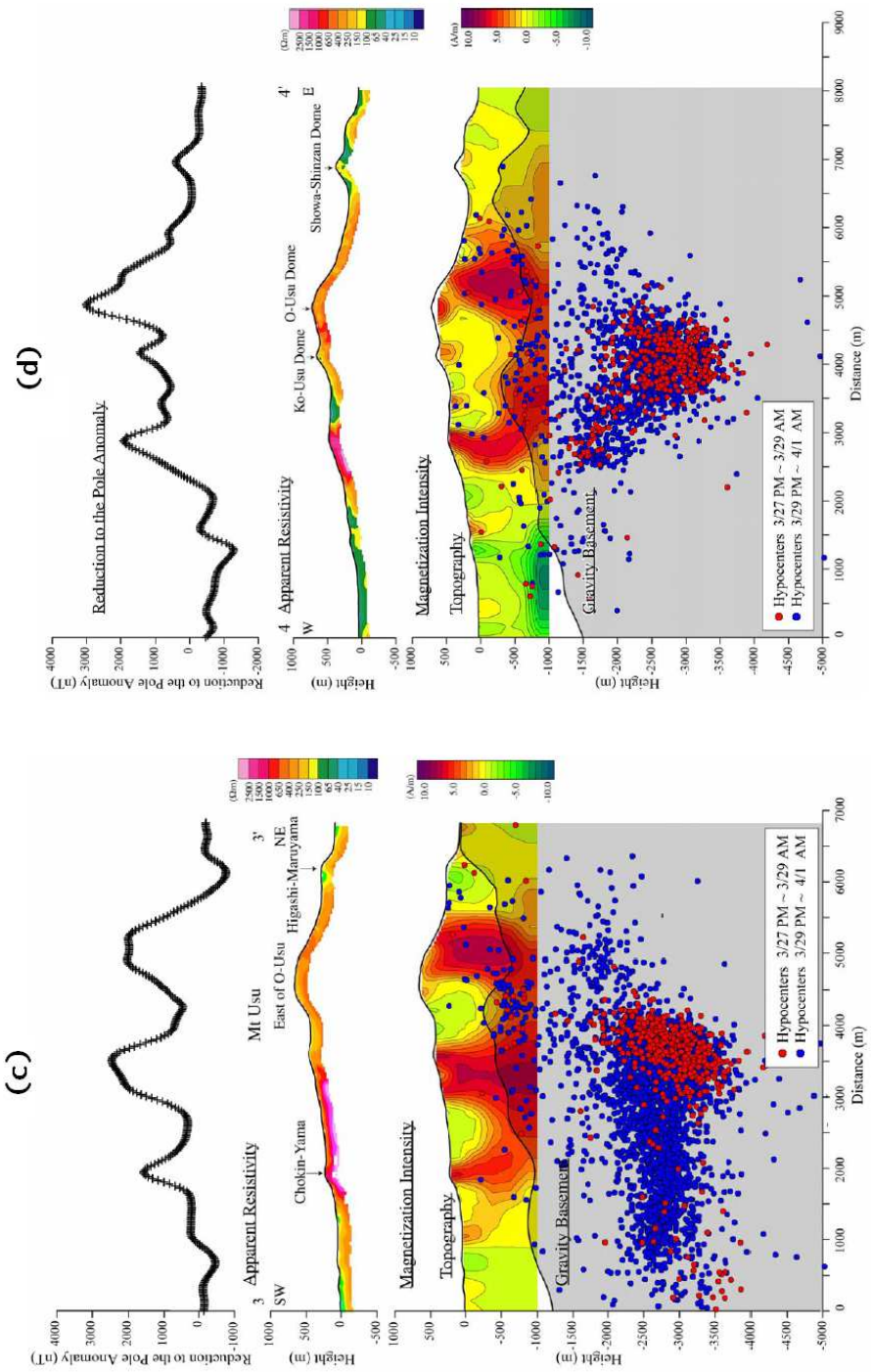

Fig. 7. (Continuued)

Figure 7*b* shows a cross-section that traverses the summit crater area, where the last eruption to occur was that in 1977–1978. Magnetisation highs (~10 A/m) occupy the main edifice of the volcano, from which the subsurface distribution of the Usu somma lava can be inferred. A magma intrusion during the 1977–1978 eruption below the Usu-Shinzan Fault, where no obvious magnetic features are seen, was proposed by a magnetotelluric (MT) survey (Matsushima et al., 2001). However, the area corresponds to a boundary of positive magnetisation (~4 A/m) and negative magnetisation (~–2 A/m). This discrepancy can be explained as follows.

According to laboratory measurements, the electrical resistivity of lava is known to be more sensitive to its temperature than to its magnetic properties. For instance, the electrical resistivity of dacite lava from Showa-Shinzan Lava Dome increases rapidly from just a few ohm-metres to several hundred ohm-metres with the decrease of the lava temperature from around 1000℃ to 700℃ (Murase, 1962), whereas the lava cannot acquire magnetisation at temperatures higher than its Curie temperature of 560℃ (Nemoto et al., 1957).

Figure 7*c* shows a cross-section that traverses Chokin-Yama, a mega block of the Zenkoji Debris Avalanche Deposit, and Higashi-Maruyama Cryptodome on the southern and north northeastern flanks of Usu Volcano, respectively. A magnetization high with a dyke-like shape was imaged below Chokin-Yama, suggesting that Chokin-Yama might in fact be a lateral volcano, rather than part of the debris avalanche deposits. We will make more detailed comments about this in discussion. On the other hand, there is a magnetisation low (~–2 A/m) on Higashi-Maruyama Cryptodome, implying that the cryptodome is composed of reversely magnetised rocks.

Figure 7*d* shows a cross-section that traverses Showa-Shinzan Lava Dome, the 1943–1945 eruption area on the eastern flank of the main volcano. Local magnetisation highs (3–5 A/m) are mapped on Usu-Shinzan Cryptodome and O-Usu Lava Dome. Meanwhile, there is a low amplitude local magnetisation high (1–2 A/m) on the Showa-Shinzan Dome. This implies that the lava dome becomes magnetised as it cools, but its magnetization is not as strong as that of the basaltic somma lava because of its dacitic composition.

Discussion

In this section, we discuss the results of the 3D imaging of magnetic anomalies in the context of magnetic properties of rocks sampled from the study area. Nemoto et al. (1957) conducted petrophysical measurements of volcanic rocks from Usu Volcano, Showa-Shinzan Dome and their surrounding areas. According to Nemoto et al. (1957), natural remanent magnetisation (NRM) intensity and magnetic susceptibility of dacite lavas from O-Usu LavaDomeare $1.32–2.09\times10^{-3}$ e.m.u./g and $0.12–0.45\times10^{-3}$ e.m.u./g, respectively. Given their density of 2.65 g/cm^3, their NRM intensity and magnetic susceptibility can be converted to 3.50–5.54 A/m and $0.32–1.19\times10^{-3}\times4\pi$ in SI, respectively. The NRM intensity and magnetic susceptibility of the Usu somma lava, with a density of 2.92 g/cm^3, are 7.50 A/m and $2.60\times10^{-3}\times4\pi$ (SI), respectively. The direction of NRM of the Takinoue Welded Tuff (Takinoue Pyroclastic Flow Deposits) is perpendicular to that of the Earth's present magnetic field.

We conducted additional petrophysical measurements of the rocks from the study area. We measured physical properties of cylindrical rock specimens including magnetic susceptibility, intensity of NRM, Q_n (Könighsberger) ratio, dry density, wet density and porosity. For the magnetic susceptibility measurement, two types of magnetic susceptibility meter were used, Model 3101A (Bison Instruments, Minneapolis, USA) and Model MS 2 (Bartington Instruments, Witney, UK). For the NRM measurement, a spinner magnetometer Model SMD-88 (SMM-85) (Natsuhara Giken, Osaka, Japan) was used. The results are summarised in Table 1.

The NRM intensity of the Usu somma lava, which constitutes the main edifice of the Usu Volcano, ranges from 5.8 A/m to 9.8 A/m with a normal magnetisation. As shown in Figure 7, magnetisation highs (7–10 A/m) are dominant on the main edifice of Usu Volcano and conform to the results of rock magnetic measurements.

According to our 3D magnetic imaging (Figure 7*c*), Chokin-Yama has magnetisation intensity as large as 6 A/m which falls in the range for rock magnetic measurements of the Usu soma lava (5.8 – 9.8 A/m in Table 1). This suggests that the mountain is a mega block of the Zenkoji Debris Avalanche Deposits and is thus composed of basaltic somma lava and its matrices.

To confirm this, we conducted further magnetic modelling. We assumed an ensemble of vertical prisms for each block with the horizontal boundaries deduced from the topographic and geologic maps (Figures 1 and 2). This approach is the same as that used by Okuma et al. (2006) when they conducted modeling of the Vulcano-Lipari volcanic complex, Italy. We fixed the top of the vertical prisms for each block as the ground surface, while allowing variations of the bottom depths.

Synthetic magnetic anomalies, which best fit the observed anomalies, were calculated by trial and error,

Table 1. Results of rock magnetic measurements for samples from the study area. The sampling locations are shown in Figure 1.

Sampling site Name	Latitude (deg.)	Longitude (deg.)	NRM Dec. (deg.)	NRM Inc. (deg.)	NRM Intensity (A/m)	Magnetic susceptibility ($\times10^{-5}$ SI)	Q_n ratio	Density ($\times10^3$ kg/m^3) Dry	Density Wet	Porosity (%)	Number of specipens	Lithology
U-1	42.54760	140.84171	15.40	74.30	9.79	3,055	9.19	2.580	2.667	8.67	25	Usu somma lava
U-2	42.54829	140.86218	5.12	58.60	5.81	1,536	11.2	2.128	2.370	24.18	49	Usu somma lava
U-3	42.56216	140.88606	174.50	–65.30	1.33	752	4.77	2.233	2.351	11.75	19	Takinoue Welded Tuff
U-4	42.56498	140.79764	–152.49	–48.61	0.63	4,171	0.43	2.682	2.724	4.17	18	Nottoko lava in Mitoyo tunnel
U-5	42.56498	140.79764	–152.29	–29.17	2.32	4,560	1.35	2.593	2.682	8.90	9	Nottoko lava in Mitoyo tunnel
U-6	42.58060	140.79910	110.18	–56.50	1.40	4,187	1.00	2.780				

Table 2. Parameters used for the magnetic modelling for Chokin-Yama and its surroundings.

Parameters	Block 1	Block 2	Block 3	Block 4
Top depth (m)	Ground surface	Ground surface	Ground surface	Ground surface
Bottom depth (m)	30m downward from the interpolated ground surface	30m downward from the interpolated ground surface	30m downward from the interpolated ground surface	30m downward from the interpolated ground surface
Total magnetisation intensity (A/m)	8.0	10.0	5.0	5.0
Inclination of total magnetisation (°)	57.0	57.0	57.0	57.0
Declination of total magnetisation (°)	–9.0	–9.0	–9.0	–9.0

also varying the rock magnetisation data. We used the term 'goodness-of-fit' (r) (Blakely, 1995, p.224) to describe how well synthetic anomalies (G) fit the observed anomalies (F): the larger the ratio, the better the fit. The goodness-of-fit (r) is defined as

$$r = \frac{\sum_{i=1}^{n} |F_i|}{\sum_{i=1}^{n} |F_i - G_i|} \qquad (6)$$

We show the result of the modelling when the goodness-of-fit (r) is 1.60 (Figure 8). The parameters used for the modeling are shown in Table 2. Four blocks were extracted referring to the topographic and geologic maps (Figure 8*a*). The bottom depth of each block was assumed to be parallel-shifted 30 m downward from the synthetic surface. This was calculated by interpolating the gaps caused by excluding topographic highs of Chokin-Yama and its surroundings including the peak of 245 m from the terrain surface (Figure 8*d*). We note that thinner blocks than the magnetisation high areas analysed by the 3D magnetic imaging can account for the observed magnetic anomalies, if there is an assumption of strong magnetization intensities (~10 A/m) for the blocks. Since these strong magnetisation intensities are comparable with the result of the rock magnetic measurements for the Usu somma lava (Table 1), there is a large possibility that the topographic highs including Chokin-Yama and its surroundings are composed of the Usu somma lava and correspond to mega blocks of the Zenkoji Debris Avalanche Deposits. Since the topographic highs lie at the second highest altitude among the hills of the debris avalanche deposits, they are inferred to be one of the last parts to have rushed down the flank of Usu Volcano. Even if they are lateral volcanoes, they would not have been formed by dacite magma but by the similar basaltic magma to the main edifice of Usu Volcano.

It is also notable that the result of the 3D magnetic imaging tends to reveal broader source distributions than the modeling assuming isolated models, even though the 3D magnetic imaging estimates the distribution of magnetisation intensity with effective source volume minimisation (equations 4 and 5).

The NRM intensity of the Takinoue Welded Tuff is 1.3 A/m, indicating a polarity reversal that is consistent with previous measurements (Nemoto et al., 1957). As explained in the previous section, a reversely magnetised area (~–2 A/m) was inferred at Higashi-Maruyama Cryptodome from the 3D magnetic imaging (Figure 7*c*). Although no reversely magnetised rocks crop out there,

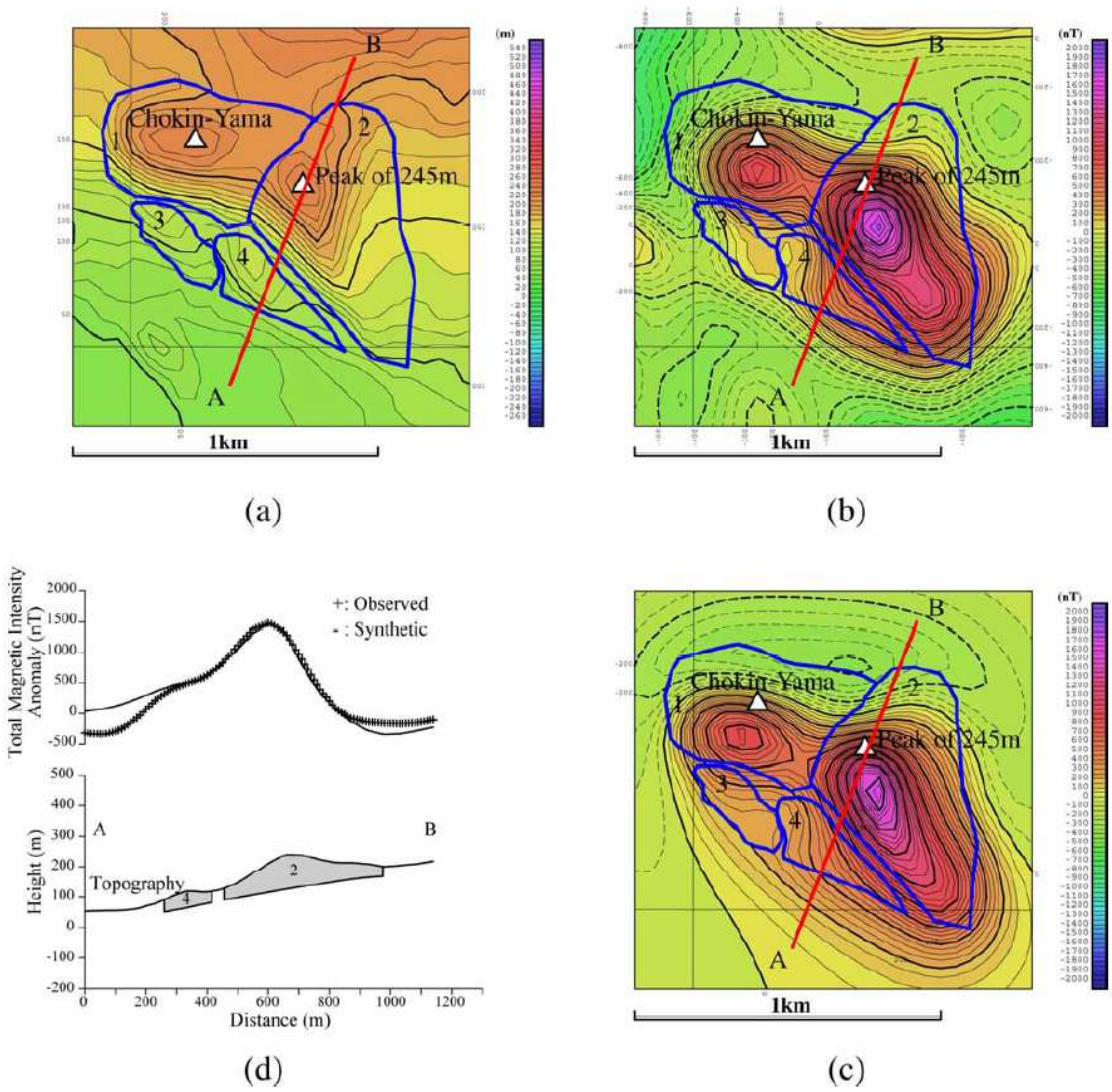

Fig. 8. Result of magnetic modelling for Chokin-Yama and its surroundings. (*a*) Topographic map of Chokin-Yama and its surroundings. Contour interval is 10 m. The profile of A-B indicates the location of the cross-section (Figure 8*d*). Thick solid lines show block boundaries. Numbers 1 to 5 denote block numbers. (*b*) Observed magnetic anomalies (total magnetic intensity) in the study area. The mean value was removed. Contour interval is 50 nT. Dashed contours indicate negative values. See also Figure 8*a*. (*c*) Synthetic magnetic anomalies in the study area. Contour interval is 50 nT. Goodness-to-fit (*r*) is 1.60. See also Figure 8*b*. (*d*) Cross-section of the observed (Figure 8*b*) and synthetic (Figure 8*c*) magnetic anomalies along the profile of A-B. See the location in Figure 8*a*.

some Takinoue Welded Tuff was recovered from drilling in a geothermal exploration well south of Showa-Shinzan Lava Dome, close to Higashi-Maruyama (Oshima and Matsushima, 1999). On the basis of these results, it is inferred that Higashi-Maruyama is underlain by Takinoue Welded Tuff.

Reversed magnetisations were also measured for the Nottoko lava sampled from the inside of Mitoyo tunnel, which was under construction when the sampling was conducted, and for the Tsukiura lava along the shoreline of the Lake Toya. This is related to reversely magnetised areas (~–10 A/m) that were assumed to exist in the north-west of the 2000 eruption area by 3D magnetic imaging. However, the intensity of NRM measured for the Nottoko lava from the inside of Mitoyo tunnel is not so strong (~–2.32 A/m). This fact leads to the deduction that more strongly magnetised rocks with a reverse polarity lie at depth, as imaged by the magnetic inversion (Figure 7*a*).

On the basis of these results, we conclude that the aeromagnetic survey has improved our understanding of the surface and subsurface distribution of the volcanic rocks that constitute the edifice and basement of Usu Volcano. However, our survey did not reveal any information about the magmas intruded during recent eruptions in 1977–1978 and 2000, though some

intrusions are suggested by other geophysical data. The intruded magmas were estimated at several hundred meters below the ground with a volume of 3×10^7 m^3 for the 2000 eruption (Murakami et al., 2001) and of 8×10^7 m^3 for the 1977–1978 eruption (Matsushima, 2003). In this case, the presence of the magma intrusion could be successfully modelled if there is a large magnetic contrast between the intrusion and its host rock. The reasons why the magma intrusions of the 2000 and 1977–1978 eruptions were not imaged properly are thought to be as follows.

The aeromagnetic survey was conducted only three months after the beginning of the 2000 eruption. This means that the intruded magma from 2000 had not cooled enough to acquire magnetisation by the time of the survey and can be regarded as non-magnetic. If such magma intruded into the magnetic host rock, it would change the magnetic structure and consequently contribute to a magnetic anomaly with a polarity opposite to that of the host rock. However, the magnetic properties of the host rock in the 2000 eruption area are not so simple, since the area lies at the boundary between the Neogene volcanic region (reversely magnetised) to the north-west and the Quaternary volcanic region (normally magnetised) to the south-east (Figure 2). Therefore, the host rock might comprise less magnetic rocks such as pyroclastic rocks and/or volcanic layers mixed with normal and reverse polarisations. Either way, the resultant magnetisation is reduced. In this case, there is insufficient magnetic contrast between the intrusion and its host rock and consequently the existence of the intrusion could not be modelled.

In the case of the 1977–1978 eruption, which occurred in the summit crater of Usu Volcano, the crater floor is composed mainly of less magnetic pyroclastic fall deposits. The intruded magma that caused the 1977–1978 eruption is inferred to have cooled enough to have acquired some magnetisation by the time the aeromagnetic survey was conducted in 2000. However the intrusion might not have been strongly magnetised since it is dacitic and still hot enough to cause the ongoing intensive geothermal activity in the crater floor. This suggests that there was also insufficient magnetic contrast between the intrusion and its host rock to change the magnetic structure and cause obvious magnetic anomalies. Consequently, it is not easy to obtain useful information associated with the volcanic activity of a volcano form a single survey.

Repeat aeromagnetic surveys are a promising way to extract temporal magnetic anomaly changes over active volcanoes. Recently such a repeat aeromagnetic survey was conducted in 2010 separated by 10 years since the initial survey, in almost the same area as the first one, but limited close to the past eruption areas (Hashimoto et al., 2011). At that time, a magnetic bird which houses a Geometrics G-858 cesium magnetometer was towed from the helicopter instead of adapting a stinger system as in the previous survey. The survey helicopter was flown at an altitude of 150–250m above the ground along the east–west survey lines spaced 100mapart. The survey lines were oriented perpendicular to the previous ones to better estimate temporal variations at cross-points of each of the lines proposed by the generalized mis-tie control method (Nakatsuka and Okuma, 2006*c*). After an intense inspection of the observed data, obvious temporal magnetic anomaly changes were confirmed in the 2000 eruption area (> +50 nT), in the summit crater area (> +70 nT) and in the Showa-Shinzan area (> +20 nT) by the crossover analysis (Nakatsuka et al., 2011; Hashimoto et al., 2011). Large temporal magnetic changes (> 50 nT/year) have also been observed by repeat magnetic measurements on the fixed ground stations in the Nishi-Yama Craters Area (Hashimoto et al., 2008). It is inferred that the magmas that intruded during recent eruptions are acquiring magnetisation by cooling and could be modelled by a 3D imaging method. More detailed studies on this matter are being conducted and will be reported in a separate paper.

Conclusions

To constrain the subsurface structure of Usu Volcano, Hokkaido Japan, we applied 3D magnetic imaging to magnetic anomalies over the volcano. These anomaly measurements were obtained from a high-resolution aeromagnetic survey conducted three months after the start of the 2000 eruption. The 3D magnetic model reveals that magnetisation highs occupy the main edifice of the Usu Volcano, which we infer to indicate the subsurface distribution of the Usu somma lava, which has a maximum thickness of 1000 m. Meanwhile, magnetisation lows (or negative anomalies) lie north-west of the Nishi-Yama Craters Area and on Higashi-Maruyama Cryptodome, which have Pliocene and Pleistocene volcanic rocks, respectively, distributed nearby. The reverse magnetisation observed at outcrops close to these sites can explain these magnetisation lows.

Although this initial survey improved our understanding of the surface and subsurface distribution of volcanic rocks that constitute the edifice and basement

of Usu Volcano, our understanding of the magnetic structure of the volcano is incomplete. No information about the magmas intruded during the recent eruptions in 1977–1978 and 2000 was obtained by the high-resolution aeromagnetic survey, though some intrusions could be inferred from other geophysical data. The small magnetic contrast between the intruded magmas and their host rocks is one of the most probable reasons. This implies that the intruded magmas had not cooled enough to become strongly magnetised by the time the survey was conducted. Consequently, it is not easy to get useful information associated with volcanic activity from a single survey. Therefore, repeat aeromagnetic survey is a promising method to extract temporal magnetic anomaly changes over active volcanoes. Recently such a repeat aeromagnetic survey was conducted in 2010, 10 years after the original survey, and obvious temporal magnetic changes were observed in the areas of recent eruptions in 2000 and 1977–1978 by the crossover analysis. This implies that the magmas intruded during recent eruptions are acquiring magnetisation by cooling and could be modelled by a 3D imaging method.

Acknowledgement

The authors are grateful to the Hokkaido Regional Environment Office, Nature Conservation Bureau, Ministry of the Environment, for permission to collect rock samples from Shikotsu-Toya National Park.

References

Blakely, R. J., 1995, *Potential theory in gravity and magnetic applications*: Cambridge University Press, 441p.

Geospatial Information Authority of Japan, 1999, Digital Map 50m Grid (Elevation), NIPPON-I, CD-ROM.

Geospatial Information Authority of Japan, 2007, Digital Map 10m Grid (Elevation of Active Volcanoes), CD-ROM.

Hashimoto, T., Hurst, T., Suzuki, A., Mogi, T., Yamaya, Y., and Tamura, M., 2008, The role of thermal viscous remanent magnetisation (TVRM) in magnetic changes associated with volcanic eruptions: insights from the 2000 eruption of Mt Usu, Japan: *Journal of Volcanology and Geothermal Research*, **176**, 610–616. doi:10.1016/j.jvolgeores.2008.05.009

Hashimoto, T., Utsugi, M., Nakatsuka, T., Okuma, S., Koyama, T., and Kanda, W., 2011, Temporal magnetic changes possibly due to cooling magmas as revealed by repeat helicopter-borne surveys over an active volcano: *Proceedings of the 10th SEGJ International Symposium*, 276–279. doi:10.1190/segj102011-001.68

Katsui, Y., Komuro, H., and Uda, T., 1985, Development of faults and growth of Usu-Shinzan Cryptodome in 1977–1982 at Usu Volcano, North Japan: *Journal of the Faculty of Science, Hokkaido University, Series 4, Geology and Mineralogy*, **21**, 339–362.

Matsushima, N., 2003, Mathematical simulation of magma-hydrothermal activity associated with the 1977 eruption of Usu volcano: *Earth, Planets, and Space*, **9**, 559–568.

Matsushima, N., 2010, Explanatory note of resistivity cross-section of Usu Volcano by magnetotelluric surveys, Integrated Geophysical Maps of Usu Volcano: *Digital Geoscience Map* P-7(CD), Geological Survey of Japan, AIST.

Matsushima, N., Oshima, H., Ogawa, Y., Takakura, S., Satoh, H., Utsugi, M., and Nishida, Y., 2001, Magma prospecting in Usu volcano, Hokkaido, Japan, using magnetotelluric soundings: *Journal of Volcanology and Geothermal Research*, **109**, 263–277. doi:10.1016/S0377-0273(00) 00320-6

Maus, S., Macmillan, S., Chernova, T., Choi, S., Dater, D., Golovkov, V., Lesur, V., Lowes, F., Lühr, H., Mai, W., McLean, S., Olsen, N., Rother, M., Sabaka, T., Thomson, A., and Zvereva, T., 2005, The 10th-generation international geomagnetic reference field: *Geophysical Journal International*, **161**, 561–565. doi:10.1111/j.1365-246X.2005.02641.x

Murakami, R., Ozawa, S., Nishimura, T., and Tada, T., 2001, A model of magma movements associated with the 2000 eruption of Usu volcano inferred by crustal deformation detected by continuous GPS and other geodetic measurements: *Journal of the Geospatial Information Authority of Japan*, **95**, 99–105.

Murase, T., 1962, Viscosity and related properties of volcanic rocks at 800_C to 1400_C: *Journal of the Faculty of Science, Hokkaido University, Series 7, Geophysics*, **1**, 487–584.

Nakatsuka, T., 1995, Minimum norm inversion of magnetic anomalies with application to aeromagnetic data in the Tanna area, Central Japan: *Journal of Geomagnetism and Geoelectricity*, **47**, 295–311. doi:10.5636/jgg.47.295

Nakatsuka, T., and Okuma, S., 2006*a*, Reduction of magnetic anomaly observations from helicopter surveys at varying elevations: *Exploration Geophysics*, **37**, 121–128. doi:10.1071/EG06121

Nakatsuka, T., and Okuma, S., 2006*b*, 3D subsurface imaging by aeromagnetic data: *Proceedings of the 115th SEGJ Conference*, 196–199.

Nakatsuka, T., andOkuma,S., 2006*c*, Crossover analysis for the aeromagnetic survey at varying elevations, and its application to extracting temporal magnetic anomaly change: *Butsuri-Tansa (Geophysical Exploration)*, **59**, 449–458. doi:10.3124/segj.59.449

Nakatsuka, T., and Okuma, S., 2009, Aeromagnetic 3D subsurface imaging with source volume minimization: *Proceedings of the 9th SEGJ International Symposium*, 6 (4pp), CD-ROM. doi:10.1190/segj092009-001.2

Nakatsuka, T., Okuma, S., and Joint Group for Usu Volcano Airborne Magnetic Survey, 2011, Magnetic anomaly change of Usu Volcano 2000–2010 detected by repeated aeromagnetic surveys with a study on the accuracy of 2000 survey altitude data: *Proceedings of the 2011 Conductivity Anomaly Research Group Meeting*, 37–44.

Nemoto, S., Hayakawa, M., Takahashi, K., and Koana, S., 1957, Report on the geological, geophysical and geochemical studies of Usu Volcano (Showa-Shinzan): *Report of the Geological Survey of Japan*, **170**, 149p+24p [English abstract].

Nishida, Y., and Miyajima, E., 1984, Subsurface structure of Usu Volcano, Japan, as revealed by detailed magnetic survey: *Journal of Volcanology and Geothermal Research*, **22**, 271–285. doi:10.1016/0377-0273(84)90005-2

Ohta, R., 1956, *Geological map of Japan 1 : 50,000*, *Abuta*: Geological Survey of Japan.

Okuma, S., Morijiri, R., Makino, M., and Nakatsuka, T., 1995, Evaluation of a high-resolution aeromagnetic survey in a volcanic region – The case of Yurihara area, northeast Japan: *Butsuri-Tansa (Geophysical Exploration)*, **48**, 316–332.

Okuma, S., Nakatsuka, T., Morijiri, R., Makino, M., Uchida, T., Ogawa, Y., Takakura, S., and Matsushima, N., 2001, Preliminary results of a highresolution aeromagnetic survey over Usu Volcano, Hokkaido, Japan: *Bulletin of the Geological Survey of Japan*, **52**, 149–154. [in Japanese with English abstract and figure captions]

Okuma, S., Nakatsuka, T., Takakura, S., and Morijiri, R., 2002, Helicopterborne EM survey over Usu Volcano, Hokkaido, Japan, with a special reference to the Usu 2000 eruption: *Bulletin of the Volcanological Society of Japan*, **47**, 533–546. [in Japanese with English abstract and figure captions]

Okuma, S., Nakatsuka, T., Morijiri, R., and Makino, M., 2003, Highresolution aeromagnetic anomaly map of Usu Volcano: *Total intensity aeromagnetic maps*, **41**, Geological Survey of Japan, AIST.

Okuma, S., Nakatsuka, T., Komazawa, M., Sugihara, M., Nakano, S., Furukawa, R., and Supper, R., 2006, Shallow subsurface structure of the Vulcano-Lipari volcanic complex, Italy, constrained by helicopterborne aeromagnetic surveys: *Exploration Geophysics*, **37**, 129–138. doi:10.1071/EG06129

Okuma, S., Nakatsuka, T., Komazawa, M., Matsushima, N., Satoh, H., Takakura, S., Ishizuka, Y., Onizawa, S., Ogawa, Y., and Mogi, T., 2010, Explanatory note of integrated geophysical maps of Usu Volcano, Integrated Geophysical Maps of Usu Volcano: *Digital Geoscience Map* P-7(CD), Geological Survey of Japan, AIST.

Onizawa, S., 2010, Explanatory note of precursory seismic activity of the Usu 2000 eruption, Integrated Geophysical Maps of Usu Volcano: *Digital Geoscience Map* P-7(CD), Geological Survey of Japan, AIST.

Oshima, H., and Matsushima, N., 1999, Preliminary report on hydrological environment in the shallow part of Usu Volcano: *Geophysical Bulletin of Hokkaido University*, **62**, 79–97.

Soya, T., Katsui, Y., Niida, K., Sakai, K., and Tomiya, A., 2007, Geological map of Usu Volcano (2nd edition): *Geological Map of Volcanoes*, **2**, Geological Survey of Japan, AIST.

Yahata, M., 2002, Fragmentation depths and its temporal variation during Usu 2000 phreatomagmatic and phreatic eruptions: *Bulletin of the Volcanological Society of Japan*, **47**, 263–278. [in Japanese with English abstract and figure captions]